www.MaterialsViews.com



# Exciton and Trion Dynamics in Bilayer $MoS_2$

*Jiajie Pei, Jiong Yang, Renjing Xu, Yong-Hui Zeng, Ye Win Myint, Shuang Zhang, Jin-Cheng Zheng, Qinghua Qin, Xibin Wang, Wugui Jiang, and Yuerui Lu**

2D transition metal dichacogenide (TMD) semiconductors,[1–10] such as molybdenum disulphide ($MoS_2$), have attracted tremendous attentions owing to their unique properties, such as strong interactions with light,[1–4] layer-dependent energy gaps,[5,6] electrically tunable exciton dynamics,[7,8] tightly bound trions,[9,10] and so on. The electronic band structure of $MoS_2$ strongly depends on the layer number and layer-stacking sequences.[11–13] Especially, monolayer $MoS_2$ owns the most distinct properties comparing to the few-layer counterparts, as there is no interlayer interaction and reduced screening effect;[14] for few-layer TMDs, interlayer interaction, screening effect, quantum confinement, and crystal symmetry jointly determine their electronic structures,[1,11–13] which gives rise to direct band gap emerging in monolayer $MoS_2$ and indirect band gap in few-layer $MoS_2$ at room temperature.[15] Most of previous studies and findings are limited to monolayers.[6,8,9] However, few-layer structures, particularly bilayer structure, are extremely important, since they offer us unique platforms to investigate the fundamental phenomena arising from the interlayer van der Waals interactions, which can enable many new optoelectronic devices based on heterostuctures.[16] Owing to the direct band nature, the photoluminescence (PL) intensity from monolayer $MoS_2$ can be electrically tuned by up to two orders of magnitude, which enables the control of exciton and trion dynamics in monolayer $MoS_2$ at room temperature;[8,9] in contrast, the PL spectra from bilayer $MoS_2$ could not be tuned by electric field at room temperature owing to its indirect band gap manner,[7] which makes the exciton and trion dynamics in bilayer $MoS_2$ still underexplored.

In this paper, we demonstrate the valley control of exciton and trion dynamics in bilayer $MoS_2$, via the comodulations by both temperature and electric field. We found that as temperature decreases from 300 to 100 K, the valley of the conduction band at Λ point (named as Λ valley) moves down relatively to the valley at K point (named as K valley) in monolayer $MoS_2$, while the Λ valley rises up relatively to the K valley in bilayer $MoS_2$ (**Figure 1**). This opposite temperature dependence of the valley movements in mono- and bilayer $MoS_2$ can significantly change the photocarrier relaxation pathways in their PL processes, which leads to more than twice faster increasing of the measured PL intensity from bilayer $MoS_2$ than that from monolayer $MoS_2$ as temperature decreases. More importantly, the rising up of the Λ valley in bilayer $MoS_2$ at low temperature offers the electrical tunability of the K–K direct PL transition, enabling the exploration of the exciton and trion dynamics in bilayer $MoS_2$. The trion binding energy of bilayer $MoS_2$ was firstly measured to be 27 meV at 83 K, which is smaller than the measured trion binding energy of 39 meV in monolayer $MoS_2$. Our findings provide insight into exciton and trion dynamics in bilayer $MoS_2$ and enable new applications in photonics and optoelectronics.[1,2,17] Moreover, the comodulation technique by both temperature and electric field provides a novel method to explore the fundamental phenomena in few-layer 2D semiconductors.

We calculated the band structures of mono- and bilayer $MoS_2$ at various temperatures (Figure 1) within density functional theory (DFT) molecular dynamics using Perdew–Wang (PW) generalized gradient approximation (GGA) based on a real-space numerical atomic orbital code.[18] From the simulation results, as temperature decreases from 300 to 100 K, the Γ peak in the valence band (named as Γ peak) of 2L $MoS_2$ significantly moves down relative to the K peak, which drives the indirect band structure of bilayer $MoS_2$ at room temperature approaching direct band structure at the temperature range of ≈50–250 K (Figure 1 and Figure S1, Supporting Information). Meanwhile, Λ valley moves down relatively to K valley in monolayer $MoS_2$, while Λ valley moves up relatively to K valley in bilayer $MoS_2$ (Figure 1a,c), which drives the direct band structure of monolayer $MoS_2$ at room temperature approaching indirect band structure at the temperature range of ≈50–210 K (Figure 1 and Figures S1

J. Pei, Prof. X. Wang
School of Mechanical Engineering
Beijing Institute of Technology
Beijing 100081, China
J. Pei, J. Yang, R. Xu, Y. W. Myint, S. Zhang, Prof. Q. Qin, Dr. Y. Lu
Research School of Engineering
College of Engineering and Computer Science
the Australian National University
Canberra, ACT 2601, Australia
E-mail: yuerui.lu@anu.edu.au
Y.-H. Zeng, Prof. W. Jiang
School of Aeronautical Manufacturing Engineering
Nanchang Hangkong University
Nanchang 330063, China
Prof. J.-C. Zheng
Department of Physics and Institute of Theoretical Physics and Astrophysics
Xiamen University
Xiamen 361005, China

DOI: 10.1002/smll.201501949

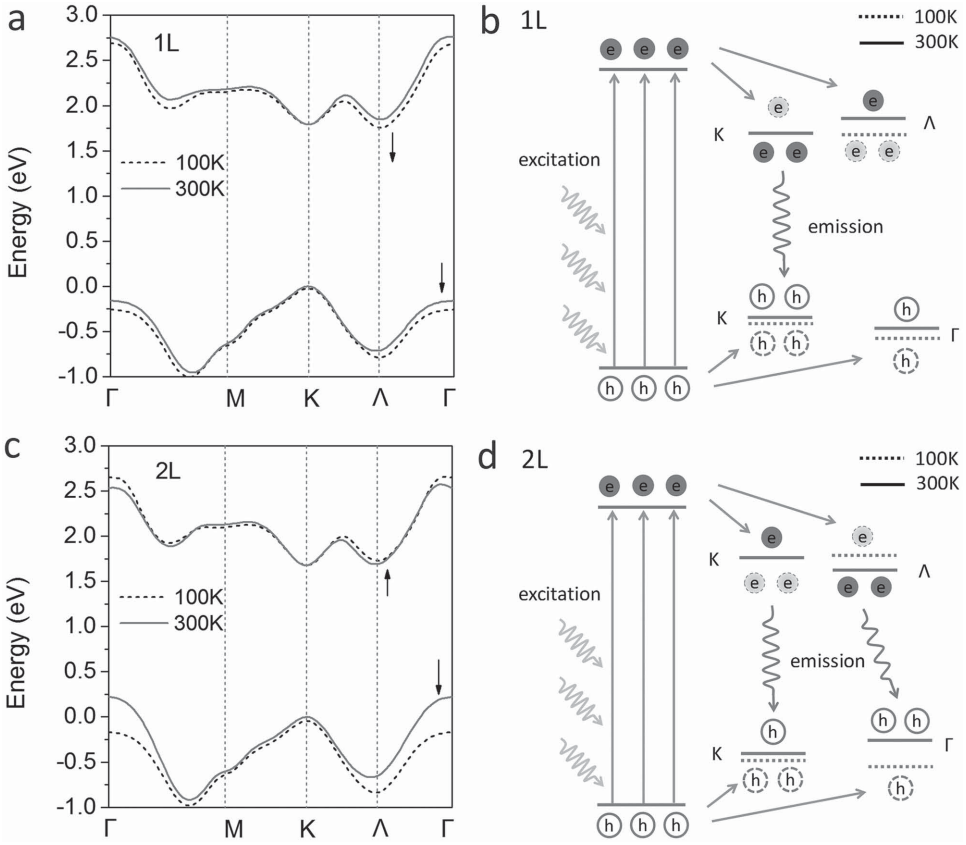


**Figure 1.** Calculated band structures of mono- and bilayer $MoS_2$ and the schematic of their photocarrier relaxation pathways at 100 and 300 K. a,c) Band structure of monolayer (labeled as "1L") and bilayer (labeled as "2L") $MoS_2$.The solid black arrows indicate the moving directions of Λ valley and Γ peak as temperature decreases (K point is fixed). b,d) Schematic of the photocarrier relaxation pathways in 1L (b) and 2L (d) $MoS_2$. The orange and green lines indicate the VBM and CBM, respectively. The green circle "e" stands for electrons and orange circle "h" stands for holes. The dashed and solid lines present the situations at 100 and 300 K, respectively.

and S2, Supporting Information). This opposite movement of the valleys with temperature can also significantly change the photocarrier relaxation pathways in mono- and bilayer $MoS_2$,[17] since photoexcited electrons and holes will always prefer the low energy states. Hence, the weight of the photoelectrons relaxed into the K valley will decrease in monolayer $MoS_2$ as temperature decreases (Figure 1b), while conversely in bilayer $MoS_2$, more portion of photoelectrons will relax into K valley at lower temperature (Figure 1d). Similarly, the holes in valence band follow the same rules as shown in Figure 1. In order to investigate this opposite temperature dependence of the photocarrier pathways, we carried out temperature dependent PL measurements on both mono- and bilayer $MoS_2$ samples as a comparison.

**Figure 2** shows the results of temperature dependent PL measurements from mono- and bilayer $MoS_2$ samples. The low temperature PL measurements were carried out with a Horiba Yvon T64000 micro-Raman/PL system equipped with a Linkam liquid nitrogen chamber, using a 532 nm green laser for excitation. In the experiment, the low temperature chamber was cooled down from room temperature (298 K) to near liquid nitrogen temperature (83 K), with a step of 30 K. It is clear to see that the PL intensity increases with the decrease of temperature for both mono- and bilayer samples, which are due to the suppressed nonradiative decays at low temperature.[17] The PL peak location shows a blue shift with the decrease of temperature, which can be explained by the Varshni relation.[19] Yet the increasing PL intensity for mono- and bilayer $MoS_2$ shows different trends. From 298 to 233 K, the PL intensity of monolayer $MoS_2$ is stronger than that of the bilayer $MoS_2$ sample, owing to the direct band gap in monolayer $MoS_2$ and the indirect band gap in bilayer $MoS_2$ at this relatively high temperature range. However, from 203 K, the PL intensity from bilayer $MoS_2$ surpasses that from monolayer and reaches almost twice the intensity from the monolayer $MoS_2$ sample at 83 K, as indicated in Figure 2c. A similar trend was also observed from another batch of mono- and bilayer $MoS_2$ samples (Figure S3, Supporting Information). At a low temperature of 83 K, the much faster rising of the PL intensity from bilayer $MoS_2$ comparing to monolayer can be explained with the tuning of band structure with decreasing temperature. More specifically, the K–K carrier recombination pathway is suppressed with the moving down of Λ valley in monolayer $MoS_2$, while the K–K carrier recombination pathway is strengthened with the rising up of the Λ valley in bilayer $MoS_2$.

In contrast to an exciton, a trion (charged exciton) has an extra charge with nonzero spin, which can be used for spin manipulation.[20,21] More importantly, the density of trions can be electrically tuned by the gate voltage, offering

  

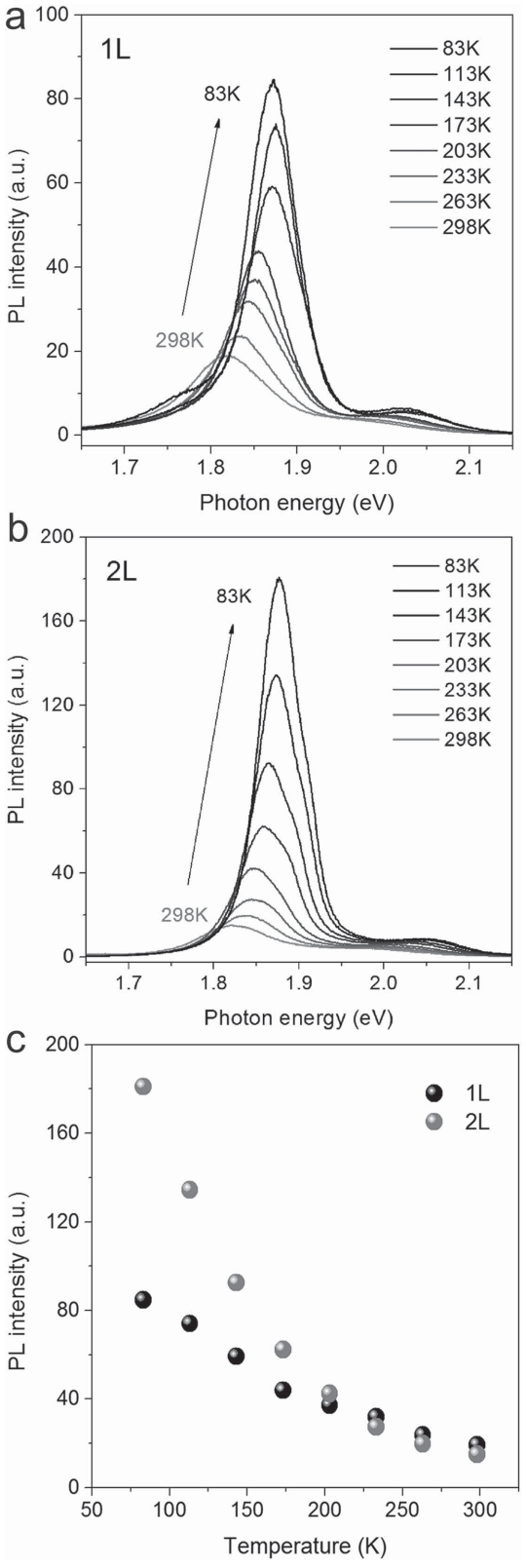


**Figure 2.** Temperature dependence of the photoluminescence (PL) from mono- and bilayer $MoS_2$. a,b) The measured PL spectra from mono- and bilayer $MoS_2$, respectively, at different temperatures ranging from 298 down to 83 K. c) PL intensity as a function of temperature for 1L and 2L $MoS_2$ samples, showing a more rapid increase of the PL intensity from 2L sample than that from1L $MoS_2$ as the temperature decreases.

remarkable optoelectronic applications.[22–26] Recently, tightly bound trions have been observed in monolayer $MoS_2$ at room temperature, which is of considerable interest for the fundamental studies of many-body interactions, such as carrier multiplication and Wigner crystallization.[27] However, trions have not been observed in bilayer $MoS_2$, since the PL spectra in bilayer $MoS_2$ could not be tuned at room temperature owing to its indirect band gap nature at room temperature. Fortunately, we could use temperature to tune the valley positions in bilayer $MoS_2$ and make its electronic band structure approaching direct band gap manner, which offers the electrical tunability of the exciton and trion dynamics in bilayer $MoS_2$ at low temperature.

Using back-gated metal–oxide–semiconductor (MOS) devices (**Figure 3**a,b), we demonstrate the tunability of exciton and trion dynamics in bilayer $MoS_2$ at low temperature, with the comodulations by both temperature and electric field. We used mechanical exfoliation to transfer[28] a $MoS_2$ flake (with mono- and bilayer $MoS_2$) onto a $SiO_2$/Si substrate (275 nm thermal oxide on $n^+$-doped silicon). The $MoS_2$ flake was placed near a gold electrode that was prepatterned on the substrate. Another thick graphite flake was similarly transferred to electrically bridge the $MoS_2$ flake and the gold electrode, forming a MOS device. This fabrication procedure kept the $MoS_2$ samples free from chemical contaminations by minimizing the post-processes after the $MoS_2$ flake was transferred. In the measurement, the gold electrode is grounded, and the $n^+$-doped Si substrate functions as a back gate providing uniform electrostatic doping in the $MoS_2$ (Figure 3b). In the experiment, we tuned the back gate voltage from 50 to –50 V. For the monolayer $MoS_2$, obvious gate-dependent PL spectra were observed at both 298 and 83 K (Figure 3c,d). In the PL spectra, the higher-energy emission peak at ≈1.92 eV is attributed to neutral exciton (A) emission, and the lower-energy emission peak at ≈1.88 eV (Figure 3c,d) is attributed to negative trion ($A^-$) emission, which is consistent with previously report.[26] $MoS_2$ sample is an n-type semiconductor owing to the initial electron doping,[26] which makes the negative trion PL peak dominant at zero back gate voltage (Figure 3 c,d). As the back gate voltage $V_g$ was changed from –50 to 50 V, positive charges were injected to monolayer $MoS_2$ layer sample and makes the doping level close to neutral at –50 V. Therefore, the exciton spectral weight was increasing with the injection of positive charges by back gate voltages and negative trions ($A^-$) will be converted to excitons (A). The conversion can be represented as $A^- + h \rightarrow A$, where $h$ represents a hole. In monolayer $MoS_2$, most photocarriers will recombine through the K–K transitions at 298 K. When temperature is down to 83 K, Λ valley slightly moves down relatively to K valley, which reduces the weight of the photoelectrons relaxed into K valley. However, as the photoelectrons still remain with a moderate amount in K valley, the conversion from exciton (A) to negative trion ($A^-$) will not be significantly influenced, so gate-dependent PL spectra could be observed from monolayer $MoS_2$ at both 298 and 83 K as shown in Figure 3c,d, respectively.

On the other hand, we did not observe obvious gate-dependent PL spectra from bilayer $MoS_2$ at 298 K

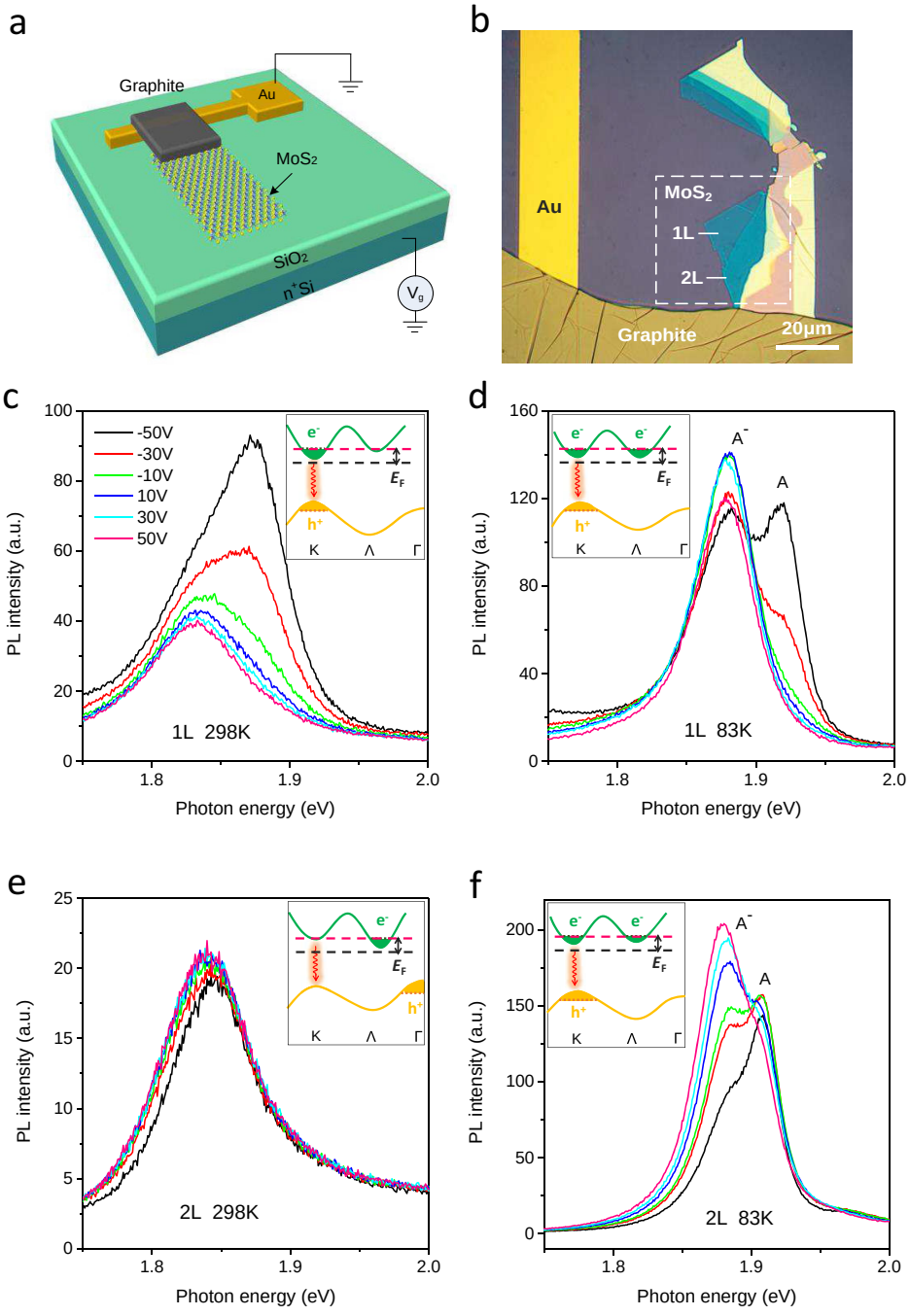


**Figure 3.** Comodulations of the PL by both temperature and electric field in mono- and bilayer $MoS_2$ samples. a) Schematic plot of a $MoS_2$ metal–oxide–semiconductor (MOS) device structure. b) Optical microscope image of the MOS device with mono- and bilayer $MoS_2$ (labeled as "1L" and "2L," respectively). c–f) Measured PL spectra from 1L and 2L $MoS_2$ samples, under different back gate voltages (from −50 to 50 V) and at temperature of 298 and 83 K, respectively. Insets show the schematic plots of the corresponding band structures with indicated quasi-Fermi level tuned by back gate.

(Figure 3e), which is consistent with previous observation.[7] At 298 K, bilayer $MoS_2$ has an indirect band gap and the quasi-Fermi level locates within the lower-energy Λ valley, but not the higher-energy K valley. The electric field from the back gate will only tune the photoelectron density within the Λ valley, but not within the K valley. Since the main PL peak in bilayer $MoS_2$ comes from the direct K–K transition, the electric field would not affect the main PL K–K emission at 298 K (Figure 3e inset). This situation changes when the MOS device was cooled down to 83 K, at which the clear gate-dependent PL spectra emerged (Figure 3f). Two clear emission peaks, located at ≈1.91 and ≈1.88 eV, respectively, could be observed via back gate modulation. The higher-energy peak at ≈1.91 eV is attributed to exciton (A) emission and

the lower-energy peak at ≈1.88 eV is attributed to the negative trion ($A^-$) emission.[8] The trion binding energy[29] is the energy difference of these two peaks A and $A^-$. The emerging gate-dependent PL spectra in bilayer $MoS_2$ at 83 K come from the rising up of the Λ valley relatively to the K valley. When the energy of Λ valley becomes comparable to that of K valley, the weight of photoelectrons relaxed to K valley will be highly enhanced (Figure 3f inset), which leads to the electrical tunability of the PL and the exciton and trion dynamics in bilayer $MoS_2$ at 83 K.

In order to investigate the detailed exciton and trion dynamics in mono- and bilayer $MoS_2$, we measured their PL spectra under various back gate voltages at different temperatures ranging from 298 down to 83 K. All the PL spectra are fitted using Lorentzian function to extract the exciton and trion components (Figures S4 and S5, Supporting Information). In monolayer $MoS_2$, the intensity of excitons exhibits a large gate dependence, while the intensity of trions approximately preserves when the back-gated voltage is changed from –50 to 50 V at 83 K (**Figure 4**a), which is consistent with previous report.[9] For bilayer $MoS_2$, the back gate voltage will have an obviously larger influence on the spectral weight of trions than that of excitons at 83 K (Figure 4b), which could be related to the initial carrier density of K valley in bilayer $MoS_2$.[17] The trion binding energies of mono- and bilayer $MoS_2$ are measured to be 39 and 27 meV at 83 K (Figure 4c,d), respectively. The lower trion binding energy in bilayer $MoS_2$ could be due to the reduced quantum confinement.[9,30] For 2L $MoS_2$ at both 298 and 263 K, the PL spectra can only be fitted using one peak and this peak is attributed to the emission of excitons, according to the temperature evolution of exciton and trion peak energies for 2L $MoS_2$ (Figure 4d and Figure S5b, Supporting Information). This is because most of the photoexcited electrons relax to the Λ valley rapidly, making the neutral excitons dominant in the K–K transition (Figure 3e inset). We find that the peak positions of exciton and trion emissions in both mono- and bilayer can be fitted well (solid lines in Figure 4d) using a standard semiconductor band gap dependence[7,31] of $E_g(T) = E_g(0) - S\hbar\omega\left[\coth\left(\frac{\hbar\omega}{2kT}\right) - 1\right]$, where $E_g(0)$ is the ground-state transition energy at 0 K, $S$ is a dimensionless coupling constant, and $\hbar\omega$ is an average phonon

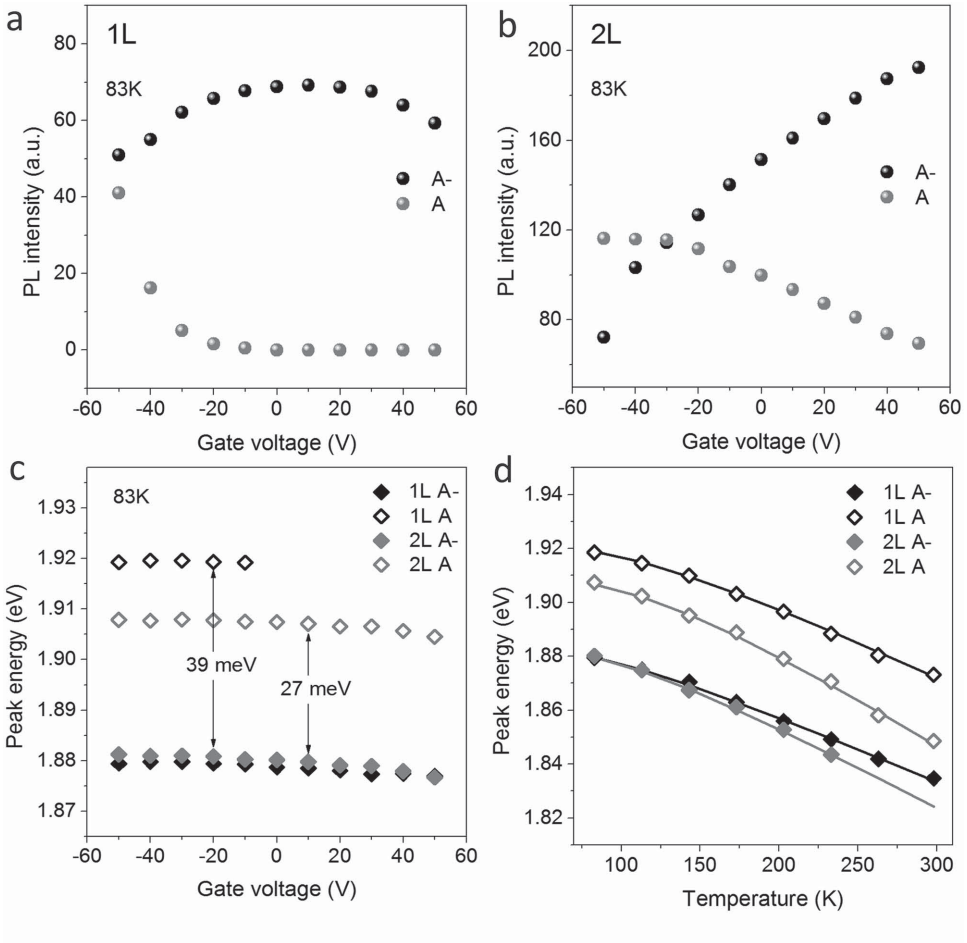


**Figure 4.** Exciton and trion dynamics in mono- and bilayer $MoS_2$, at different back gate voltages and temperatures. a,b) PL intensity of emission peaks from excitons ("A") and trions ("$A^-$") as a function of gate voltages, from 1L (a) and 2L (b) $MoS_2$ at 83 K. c) PL peak energy of "A" and "$A^-$" emissions as a function of gate voltages for 1L and 2L $MoS_2$ at 83 K. d) PL peak energy as a function of temperature. For 2L, the "A" peak can only be fit out below 233 K. All the peaks are fit to Lorentzians by multipeak fitting (see the Supporting Information). The solid lines are the fitting curves using a standard semiconductor band gap dependence of $E_g(T) = E_g(0) - S\hbar\omega\left[\coth\left(\frac{\hbar\omega}{2kT}\right) - 1\right]$, where $E_g(0)$ is the ground-state transition energy at 0 K, $S$ is a dimensionless coupling constant, and $\hbar\omega$ is an average phonon energy.

energy. From the fits, we extract for excitons (trions) the $E_g$ = 1.921 (1.883) eV, $S$ = 1.668 (1.488), $\hbar\omega$ = 26.92 (21.29) meV in monolayer $MoS_2$ and $E_g$ = 1.909 (1.883) eV, $S$ = 2.223 (1.887), $\hbar\omega$ = 28.99 (23.81) meV in bilayer $MoS_2$.

In conclusion, we successfully used comodulation technique by both temperature and electric field to probe the exciton and trion dynamics in bilayer $MoS_2$. From numerical calculations, we show that the band structure evolution of bilayer $MoS_2$ is from indirect at room temperature toward direct band structure as temperature decreases, while monolayer $MoS_2$ shows an adverse trend. This opposite temperature dependence of the band structure evolution in mono- and bilayer $MoS_2$ can significantly change the photocarrier relaxation pathways in their PL processes, which leads to more than twice faster increasing of the measured PL intensity from bilayer $MoS_2$ than that from monolayer $MoS_2$ as temperature decreases. More importantly, this indirect-to-direct transition trend in bilayer $MoS_2$ at low temperature provides the electrical tunability of the K–K direct PL transition, which enables the exploration of exciton and trion dynamics in bilayer $MoS_2$. The trion binding energy of bilayer $MoS_2$ was then measured to be 27 meV at 83 K, which is smaller than the measured trion binding energy of 39 meV in monolayer $MoS_2$. Our results pave a new way to enable new excitonic devices using bilayer $MoS_2$.

## Experimental Section

*Device Fabrication and Characterization*: Mechanical exfoliation was used to transfer a $MoS_2$ flake onto a $SiO_2$/Si substrate (275 nm thermal oxide on $n^+$-doped silicon), near a prepatterned Au electrode. The Au electrodes were patterned by conventional photolithography, metal deposition, and lift-off processes. Another thick graphite flake was similarly transferred to electrically bridge the $MoS_2$ flake and the Au electrode, forming a MOS device. All PL measurements were conducted using a T64000 micro-Raman system equipped with a charge-coupled device (CCD) and InGaAs detectors, along with a 532 nm Nd:YAG laser as the excitation source. For low temperature measurements, the sample was placed into a microscope-compatible chamber with a low temperature controller (liquid nitrogen as the coolant).The electrical bias was applied using a Keithley 4200 semiconductor analyser.

*Trion Binding Energy Extraction*: The binding energies of excions and trions are extracted from the measured PL spectra using multipeak Lorentz fitting, which has been successfully used by Shan and co-workers[9] and Xu and co-workers.[29] Through Lorentz fitting, we can clearly see two peaks in each measured PL spectra. The higher-energy peak (A) is attributed to the neutral exciton emission, and the lower-energy peak ($A^-$) is due to the trion emission.[9,26] From the gate-dependence of these two peaks, we know the trion is negatively charged trion. The trion binding energy is the energy difference of these two peaks A and $A^-$.

*Band Structure Simulation*: The band structures of 1–2 L $MoS_2$ were calculated at different temperatures within DFT molecular dynamics calculation using PW generalized gradient approximation based on a real-space numerical atomic orbital code.[18] A double numerical polarized basis set was used with a *k*-point set of 25 × 25 × 1. All electrons are included in the calculation. A vacuum space of at least 30 Å was kept to avoid mirror interactions. The temperature dependence of the electronic structure is based on modeling the effects of thermal lattice expansion and the electron–phonon interaction. Before performing the DFT molecular dynamics calculation, the total number of particles, the system's volume, and the absolute temperature become constant and the system reaches an equilibrium state, after 10 ps relaxation (called the canonical NVT ensemble). At a certain temperature, molecular dynamics simulations at this temperature are conducted first to determine the lattice parameters; and then band structure is calculated using ab initio method based on the lattice parameters.

## Supporting Information

*Supporting Information is available from the Wiley Online Library or from the author.*

## Acknowledgements

*J. Pei, J. Yang, and R. Xu contributed equally to this work. The authors would like to thank Prof. Chennupati Jagadish and Prof. Barry Luther-Davies and from The Australian National University, for their facility support. The authors acknowledge financial support from ANU Ph.D. student scholarship, China Scholarship Council, National Natural Science Foundation of China (Grant No. 11162014), Australian Research Council and ANU Major Equipment Committee.*

[1] L. Britnell, R. M. Ribeiro, A. Eckmann, R. Jalil, B. D. Belle, A. Mishchenko, Y.-J. Kim, R. V. Gorbachev, T. Georgiou, S. V. Morozov, A. N. Grigorenko, A. K. Geim, C. Casiraghi, A. H. C. Neto, K. S. Novoselov, *Science* **2013**, *340*, 1311.
[2] G. Eda, S. A. Maier, *ACS Nano* **2013**, *7*, 5660.
[3] J. Yang, Z. Wang, F. Wang, R. Xu, J. Tao, S. Zhang, Q. Qin, B. Luther-Davies, C. Jagadish, Z. Yu, Y. Lu, *Light Sci. Appl.* **2014**, *6200*, 1411.
[4] M.-L. Tsai, S.-H. Su, J.-K. Chang, D.-S. Tsai, C.-H. Chen, C.-I. Wu, L.-J. Li, L.-J. Chen, J.-H. He, *ACS Nano* **2014**, *8*, 8317.
[5] J. K. Ellis, M. J. Lucero, G. E. Scuseria, *Appl. Phys. Lett.* **2011**, *99*, 261908.
[6] A. Splendiani, L. Sun, Y. Zhang, T. Li, J. Kim, C. Y. Chim, G. Galli, F. Wang, *Nano Lett.* **2010**, *10*, 1271.
[7] A. K. M. Newaz, D. Prasai, J. I. Ziegler, D. Caudel, S. Robinson, R. F. Haglund Jr., K. I. Bolotin, *Solid State Commun.* **2013**, *155*, 49.
[8] J. S. Ross, P. Klement, A. M. Jones, N. J. Ghimire, J. Yan, D. G. Mandrus, T. Taniguchi, K. Watanabe, K. Kitamura, W. Yao, D. H. Cobden, X. Xu, *Nat. Nanotechnol.* **2014**, *9*, 268.
[9] K. F. Mak, K. He, C. Lee, G. H. Lee, J. Hone, T. F. Heinz, J. Shan, *Nat. Mater.* **2013**, *12*, 207.
[10] J. Yang, T. Lü, Y. W. Myint, J. Pei, D. Macdonald, J.-C. Zheng, Y. Lu, *ACS Nano* **2015**, *9*, 6603.
[11] Q. H. Wang, K. Kalantar-Zadeh, A. Kis, J. N. Coleman, M. S. Strano, *Nat. Nanotechnol.* **2012**, *7*, 699.
[12] X. Yin, Z. Ye, D. A. Chenet, Y. Ye, K. O'Brien, J. C. Hone, X. Zhang, *Science* **2014**, *344*, 488.
[13] K. F. Mak, K. He, J. Shan, T. F. Heinz, *Nat. Nanotechnol.* **2012**, *7*, 494.

  

[14] T. Cheiwchanchamnangij, W. R. L. Lambrecht, *Phys. Rev. B* **2012**, *85*, 205302.
[15] A. Splendiani, L. Sun, Y. Zhang, T. Li, J. Kim, C.-Y. Chim, G. Galli, F. Wang, *Nano Lett.* **2010**, *10*, 1271.
[16] A. K. Geim, I. V. Grigorieva, *Nature* **2013**, *499*, 419.
[17] D. Kozawa, R. Kumar, A. Carvalho, K. Kumar Amara, W. Zhao, S. Wang, M. Toh, R. M. Ribeiro, A. H. Castro Neto, K. Matsuda, G. Eda, *Nat. Commun.* **2014**, DOI: 10.1038/ncomms5543.
[18] B. Delley, *J. Chem. Phys.* **1990**, *92*, 508.
[19] Y. P. Varshni, *Physica* **1967**, *34*, 149.
[20] C. Galland, A. Imamo lu, *Phys. Rev. Lett.* **2008**, *101*, 157404.
[21] X. Xu, W. Yao, D. Xiao, T. F. Heinz, *Nat. Phys.* **2014**, *10*, 343.
[22] V. I. Klimov, A. A. Mikhailovsky, S. Xu, A. Malko, J. A. Hollingsworth, C. A. Leatherdale, H.-J. Eisler, M. G. Bawendi, *Science* **2000**, *290*, 314.
[23] S. G. Carter, V. Birkedal, C. S. Wang, L. A. Coldren, A. V. Maslov, D. S. Citrin, M. S. Sherwin, *Science* **2005**, *310*, 651.
[24] G. D. Scholes, G. Rumbles, *Nat. Mater.* **2006**, *5*, 683.
[25] A. A. High, E. E. Novitskaya, L. V. Butov, M. Hanson, A. C. Gossard, *Science* **2008**, *321*, 229.
[26] K. Kheng, R. T. Cox, M. Y. d' Aubigné, F. Bassani, K. Saminadayar, S. Tatarenko, *Phys. Rev. Lett.* **1993**, *71*, 1752.
[27] E. Wigner, *Phys. Rev.* **1934**, *46*, 1002.
[28] A. Castellanos-Gomez, M. Buscema, R. Molenaar, V. Singh, L. Janssen, H. S. J. v. d. Zant, G. A. Steele, *2D Mater.* **2014**, *1*, 011002.
[29] J. S. Ross, S. Wu, H. Yu, N. J. Ghimire, A. M. Jones, G. Aivazian, J. Yan, D. G. Mandrus, D. Xiao, W. Yao, X. Xu, *Nat. Commun.* **2013**, *4*, 1474.
[30] A. Thilagam, *Phys. Rev. B* **1997**, *55*, 7804.
[31] K. P. O'Donnell, X. Chen, *Appl. Phys. Lett.* **1991**, *58*, 2924.

Received: July 2, 2015
Revised: August 31, 2015
Published online: November 6, 2015